J. Plasma Physics (2008), *vol.* 00, *part* 0, *pp.* 1–12. © 2008 Cambridge University Press 1
DOI: 10.1017/S0963548301004989 Printed in the United Kingdom

Simulations of 2D magnetic electron drift vortex mode turbulence in plasmas

D A S T G E E R S H A I K H and P K S H U K Ł A †

Institute of Geophysics and Planetary Physics (IGPP),
University of California, Riverside, CA 92521. USA.
Email:dastgeer@ucr.edu
†Institut für Theoretische Physik IV, Fakultät für Physik und Astronomie,
Ruhr-Universität Bochum, D-44780 Bochum, Germany
Email: ps@tp4.rub.de

(Received 31 March 2008; Revised on 11 April 2008)

Abstract. Simulations are performed to investigate turbulent properties of nonlinearly interacting two-dimensional (2D) magnetic electron drift vortex (MEDV) modes in a nonuniform unmagnetized plasma. The relevant nonlinear equations governing the dynamics of the MEDV modes are the wave magnetic field and electron temperature perturbations in the presence of the equilibrium density and temperature gradients. The important nonlinearities come from the advection of the electron fluid velocity perturbation and the electron temperature, as well as from the nonlinear electron Lorentz force. Computer simulations of the governing equations for the nonlinear MEDV modes reveal the generation of streamer-like electron flows, such that the corresponding gradients in the direction of the inhomogeneities tend to flatten out. By contrast, the gradients in an orthogonal direction vary rapidly. Consequently, the inertial range energy spectrum in decaying MEDV mode turbulence exhibits a much steeper anisotropic spectral index. The magnetic structures in the MEDV mode turbulence produce nonthermal electron transport in our nonuniform plasma.

1. Introduction

About a quarter century ago, several authors [1, 2, 3] predicted the existence of the magnetic-electron-drift vortex (MEDV) mode in a nonuniform unmagnetized plasma because of its possible importance in laser fusion as well as in nonstationary processes in laboratory plasmas. The MEDV mode is purely magnetic and has negligible density and electrostatic potential perturbations in an inhomogeneous plasma with fixed ion background. When the equilibrium electron density and electron temperature gradients are simultaneously present, the MEDV mode gets unstable [2, 3] because of a first order baroclinic force, which can enhance the wave magnetic field and electron temperature perturbations if the electron temperature gradient is sufficiently large in comparison with the density gradient. Large amplitude MEDV modes are subjected to parametric instabilities [4, 5] involving the decay and modulational interactions [6, 7, 8]. Due to the parametric processes the magnetic energy of the MEDV modes is redistributed among other modes in plasmas.

In their classic paper, Nycander *et al.* [9] derived a pair of equations governing the

dynamics of nonlinearly interacting MEDV modes. It turns out that the nonlinear mode coupling equations contain the intrinsic Jacobean nonlinearities arising from the advection of the electron fluid velocity and electron temperature perturbations, as well as the nonlinear Lorentz force. These nonlinearities are responsible for the formation of coherent magnetic structures in the form of a dipolar vortex [10, 11] and a vortex street [12].

Recently, there has been a renewed interest in the study of MEDV mode turbulence [12, 13]. Specifically, Jucker and Pavlenko [12] and Andrushchenko *et al.* [13] have presented analytical studies of the generation of large-scale magnetic fields (magnetic streamers) via the modulational instability of coherent and partially incoherent MEDV modes. The use of a quasi-linear theory also reveals the shearing of micro-turbulence by the electron flows and the corresponding electron diffusion in the presence of zonal magnetic fields and magnetic streamers [13].

In this paper, we present results of computer simulations of 2D nonlinearly interacting MEDV modes whose dynamics is governed by the nonlinear equations in Ref. [10]. Needless to say, we numerically solve the coupled equations for the wave magnetic field and the electron temperature perturbation in order to investigate the formation of magnetic and temperature fluctuation structures, as well as the associated turbulent spectra and the resultant electron transport in the magnetic structures.

2. 2D nonlinear equations

We consider a nonuniform plasma in the presence of the equilibrium density and electron temperature gradients. The latter, which are along the x axis in a Cartesian coordinate system, are maintained by the external sources, such as the dc electric field E_{0x}. The dynamics of the MEDV mode in our nonuniform plasma is governed by the electron momentum equation

$$\left(\frac{\partial}{\partial t}+\mathbf{u}\cdot\nabla\right)\mathbf{u}+\frac{e}{m}\left(\mathbf{E}+\frac{1}{c}\mathbf{u}\times\mathbf{B}\right)+\frac{1}{mn}\nabla(nT)=0, \tag{1}$$

the electron energy equation

$$\left(\frac{\partial}{\partial t}+\mathbf{u}\cdot\nabla\right)T+(\gamma-1)T\nabla\cdot\mathbf{u}=0, \tag{2}$$

the Faraday law

$$\nabla\times\mathbf{E}=-\frac{1}{c}\frac{\partial\mathbf{B}}{\partial t}, \tag{3}$$

and the Ampèrés law

$$\nabla\times\mathbf{B}=-\frac{4\pi en\mathbf{u}}{c}, \tag{4}$$

where $\mathbf{u}$ is the electron fluid velocity, T is the electron temperature, e is the magnitude of the electron charge, m is the electron mass, c is the speed of light in vacuum, $\gamma(=2/3)$ is the adiabatic index (the ratio of the specific heat), and $\mathbf{E}$ and $\mathbf{B}$ are the electric and magnetic fields, respectively. The displacement current in (4) has been neglected since the MEDV mode phase speed is much smaller than c. The assumption of immobile is justified as long as the MEDV mode frequency is larger than the ion plasma frequency.

Taking the curl of (1), using (3) and (4) and letting $\mathbf{B}=\hat{\mathbf{z}}B$, $T=T_0(x)+T_1$,

where $\hat{\mathbf{z}}$ is the unit vector along the z axis and $T_1(\ll T_0)$ is a small temperature fluctuation in the equilibrium value $T_0(x)$, we obtain [10]

$$\frac{\partial}{\partial t}\left(B-\lambda^2\nabla^2 B\right)+\beta\frac{\partial T_1}{\partial y}+\frac{e\lambda^4}{mc}[B,\nabla^2 B], \tag{5}$$

where $\beta = cK_n/e$, $K_n = \partial \ln n(x)/\partial x$, $\lambda = c/\omega_p$, and $\omega_p = (4\pi ne^2/m)^{1/2}$ is the electron plasma frequency. We have denoted $\nabla^2 = (\partial^2/\partial x^2)+(\partial^2/\partial z^2)$ and $[F,G] = \hat{\mathbf{z}}\times\nabla F\cdot\nabla F$ represents the Jacobean nonlinearity.

The electron energy equation (2) is written as

$$\frac{\partial T_1}{\partial t}+\alpha\frac{\partial B}{\partial y}+\frac{e\lambda^2}{mc}[B,T]=0, \tag{6}$$

where $\alpha = \lambda^2(eT_0/mc)[(2/3)K_n - K_T]$, and $K_T = |\partial \ln T_0/\partial x|$.

In the linear limit, we neglect the nonlinear terms in (5) and (6), and by assuming that B and T_1 are proportional to $\exp(-i\omega t + i\mathbf{k}\cdot\mathbf{r})$, we Fourier transform and combine the resultant equations to obtain the MEDV mode frequency

$$\omega = k_y\sqrt{\alpha\beta/(1+k^2\lambda^2)}, \tag{7}$$

where $\alpha\beta = V_T^2\lambda^2 K_n[(2/3)K_n - K_T]$ and $V_T = (T/m)^{1/2}$ is the electron thermal speed. Furthermore, $k^2 = k_y^2 + k_x^2$ and $k_y(k_x)$ is the component of the wave vector $\mathbf{k}$ along the $y(x)$ axis. The wavelength of the MEDV mode is assumed to be much smaller than K_n^{-1} and K_T^{-1}. Equation (7) reveals that for $k^2\lambda^2 \ll 1$, the phase speed ω/k_y of the MEDV mode is constant, while for $k^2\lambda^2 \gg 1$, we have $\omega = (k_y/k)\sqrt{\alpha\beta/\lambda^2}$. The latter indicates frequency condensation at $k_x \gg k_y$.

Equations (5) and (6) admit the energy integral

$$E = \int [B^2 + \lambda^2(\nabla B)^2 + (\beta/\alpha)T_1^2]dxdy. \tag{8}$$

The total energy above comprises the magnetic field, magnetic field vorticity and temperature energies. The energy integral (8) is used to check the numerical validity of our code, which must be preserved under ideal conditions.

3. Simulation results

We suitably normalize (e.g. t by ω_p^{-1}, ∇ by λ^{-1}, B by $mc\omega_p/e$, T_1 by T_0) (5) and (6) and investigate numerically the properties of 2D localized magnetic structures, as well as examine the associated magnetic turbulence spectrum and nonthermal cross-field electron transport caused by the magnetic structures.

We have developed a code to integrate the normalized (as mentioned above) equations (5) and (6). The temperature fluctuaion is reinforced due to nonlinear couplings between random set of magnetic field fluctuations and an initial temperature perturbation, while enhanced temperature fluctuations drive magnetic field fluctuations linearly due to the baroclinic force. The nonlinear interactions between MEDV magnetic fields keep mainitianing the resulting magnetic structures. Our numerical code employs a doubly periodic spectral discretization of magnetic field and temperature fluctuations in terms of its Fourier components, while nonlinear interactions are deconvoluted back and forth in real and Fourier spectral spaces. The time integration is performed by using the Runge-Kutta 4th order method. A fixed time integration step is used. The conservation of energy (8) is used to

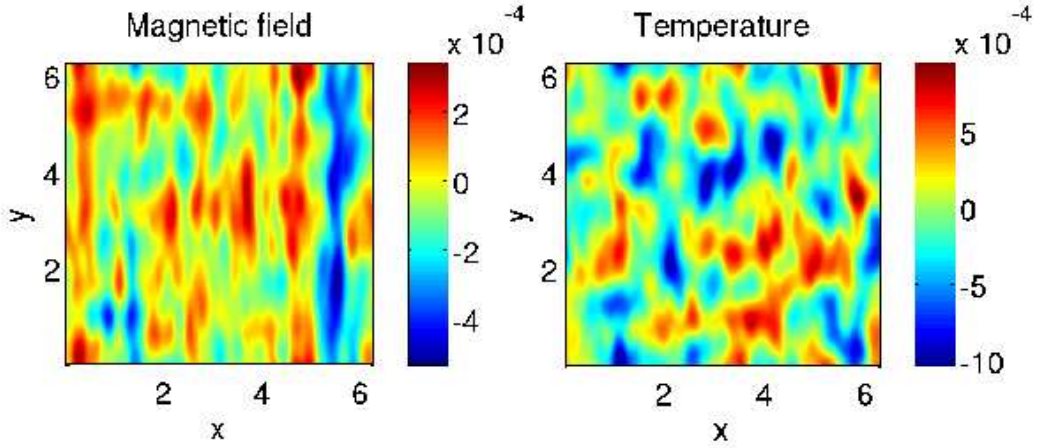

Figure 1. Formation of streamer-like flows in nearly steady-state magnetic field fluctuations. The temperature fluctuation is predominantly nearly isotropic, but some eddies are aligned in the direction of the background inhomogeniety. Numerical resolution is 512^2, box dimension is $2\pi \times 2\pi$, $\alpha = \beta = 1.0$.

check the numerical accuracy and validity of our numerical code during the nonlinear evolution of the magnetic field and temperature fluctuations. Varying spatial resolution (from 128^2 to 512^2), time step $(10^{-2}, 5 \times 10^{-3}, 10^{-3})$, constant values of $K_n \lambda V_T^2/c^2 = 0.1$ and $(2/3)K_n\lambda - K_T\lambda = 0.1$ are used to ensure the accuracy and consistency of our nonlinear simulation results. We also make sure that the initial fluctuations are isotropic and do not influence any anisotropy during the evolution. Anisotropy in the evolution can however be expected from a $k_y = 0$ mode that is excited as a result of the nonlinear interactions between the finite frequency MEDV modes.

The magnetic and temperature fluctuations are initialized by using a uniform isotropic random spectral distribution of Fourier modes concentrated in a smaller band of wave number ($k < 0.1\ k_{max}$). While spectral amplitude of the fluctuations is random for each Fourier coefficient; it follows a k^{-1} or k^{-2} scaling. Note again that our final results do not depend on the choice of the initial spectral distribution. The spectral distribution set up in this manner initializes random scale turbulent fluctuations. Since there is no external driving mechanism considered in our simulations, turbulence evolves freely under the influence of self-consistent instability. Note however that driven turbulence in the context of the MEDV mode will not change inertial range spectrum to be described here.

The nonlinear evolution of the magnetic and electron temperature fluctuations is governed typically by different nonlinearities in the two dynamical equations (5) and (6). To understand the characteristics of the nonlinear interactions in our MEDV turbulence model, it is interesting to compare it with that of the Hasegawa-Mima-Wakatani (HMW) model [14, 15, 16, 17] describing the electrostatic drift waves in an inhomogeneous magnetoplasma. For instance, the generalized magnetic field vorticity is driven by $\hat{z} \times \nabla B \cdot \nabla \nabla^2 B$ nonlinearity. The latter is similar to the ion polarization drift nonlinearity $\hat{z} \times \nabla \phi \cdot \nabla \nabla^2 \phi$, where ϕ is the electrostatic potential, in a pseudo-3D HMW equation and signifies the Reynolds stress forces that play a critical role in the formation of zonal-flows [8]. Analogously, one can expect the nonlinear generation of electron flows in our MEDV model. The nonlinearity

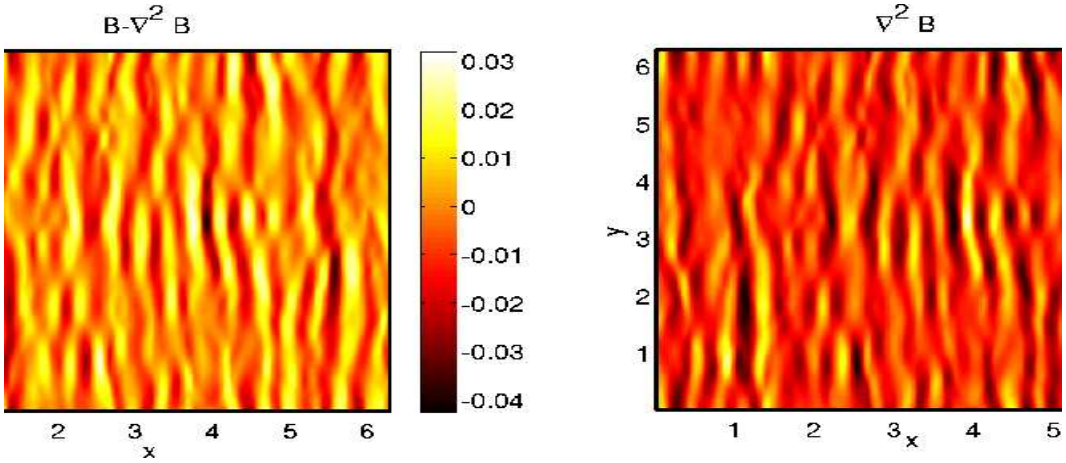

Figure 2. Formation of relatively smaller scales streamer-like flows in generalized and magnetic field vorticity fluctuations corresponding to the magnetic field structures shown in Fig (1). As expected, spectra of the latter contain smaller scales with increasingly dominated $k_y \approx 0$ modes.

in the temperature perturbation equation (6) is $\hat{z} \times \nabla T_1 \cdot \nabla B$, which is akin to a diamagnetic nonlinear term in the HMW model. The role of this nonlinearity has traditionally been identified as a source of suppressing the intensity of the nonlinear flows in the drift wave turbulence. Nevertheless, the presence of the linear inhomogenous background in both the equations can modify the nonlinear mode coupling interactions in a subtle manner. Our objective here is to understand the latter in the context of the MEDV turbulent processes. The initial isotropic and homogeneous spectral distribution in magnetic field and temperature fluctuations, as described above, evolve dynamically following the set of equations (5) and (6). The spectral magnetic energy from large scale eddies migrates towards the smaller eddies following the Richardson's cascade law. In configurational space, this essentially corresponds to breaking up the larger eddies into the smaller ones. Consequently, the mode coupling interactions in the Fourier space follow a Kolmogorov-type phenomenology in that spectral transfer, which predominantly occurs in the local k-space in the inertial range MEDV mode turbulence. During this process, each Fourier modes in the inertial range spectrum obey the vector triad constraints imposed by the vector relation $\mathbf{k} + \mathbf{p} = \mathbf{q}$. These nonlinear interactions involve the neighboring Fourier components $(\mathbf{k}, \mathbf{p}, \mathbf{q})$ that are excited in the local inertial range turbulence. The mode coupling interaction during the nonlinear stage of evolution leads to the formation of streamer-like structures in the magnetic field fluctuations associated with $k_y \approx 0, k_x \neq 0$. This is shown in Fig (1). Note that the streamer-like structures are similar to the zonal flows but contain a rapid k_x variations, thus the corresponding frequency is relatively large. The temperature fluctuations in Fig (1), on the other hand, depict an admixture of isotropically localized turbulent eddies and a few stretched along the direction of the background inhomogeneity. We have performed a number of simulations to verify the consistency of our results in a strong turbulence regime.

Figure (2) exhibits highly anisotropic nonlinear structures associated with magnetic field vorticity ($\nabla^2 B$) and generalized magnetic field vorticity ($B - \nabla^2 B$). These structures, consistent with Fig (1), vary along the x direction and contain

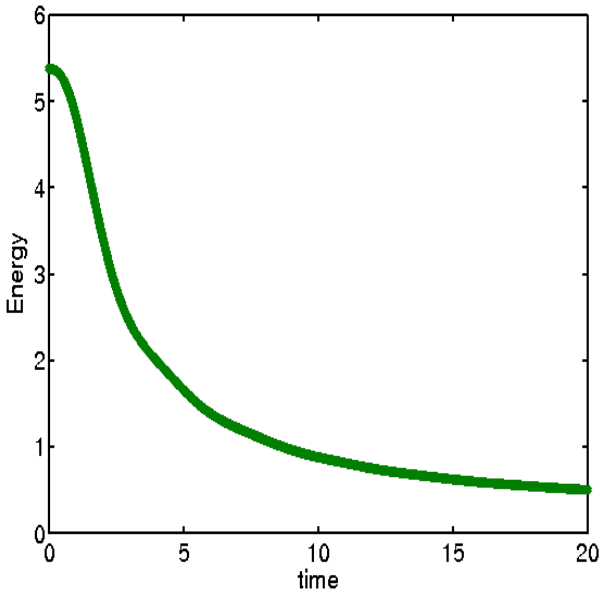

Figure 3. Evolution of the total energy in the MEDV mode turbulence. A decay can be observed owing to the presence of small scale dissipation where much of the turbulent energy is concentrated. The inclusion of dissipation not only damps the smaller scales, but it also terminates the cascade processes that results in an enhanced inertial range MEDV mode spectrum.

almost negligible gradients along the direction of inhomogeneity. The vorticities are increasingly dominated by nonlinearly generated $k_y \approx 0$ modes. The mode structures in Fig (2) comprises elongated (along the y direction) smaller scale eddies because their spectra are propotional to k^2 and $1 + k^2$, respectively.

4. Evolution of energy in the MEDV mode turbulence

The formation of relatively smaller scale fluctuations in the steady state MEDV mode turbulence (as displayed in Figs (1) and (2)) implies essentially that the inertial range turbulent spectrum is dominated by the higher Fourier modes. This is a characteristic of the forward cascade processes in that the energy containing large scales eddies transfer turbulent energy to the adjacent smaller scale until the process of energy migration is terminated by dissipative processes. To investigate the MEDV mode turbulent spectrum, we therefore include dissipation (arising from the plasma resistivity and electron thermal conduction involving electron-ion collisions) in the dynamical equations (5) and (6) to damp smaller scales and thus terminate the inertial range cascades. Note however that nonlinear interactions, in the absence of dissipation, conserves the total energy.

It is worth emphasising here that the two-component (i.e. in B and T) system of equations describing 2D MEDV mode turbulence is characteristically different from the usual 2D drift wave or Euler turbulence systems, especially in terms of the nonlinear evolution. The presence of large scale structures have been routinely observed in the latter. One of the reasons is the inverse cascade processes that migrate spectral energy from the smaller to larger Fourier modes. By contrast, in 2D

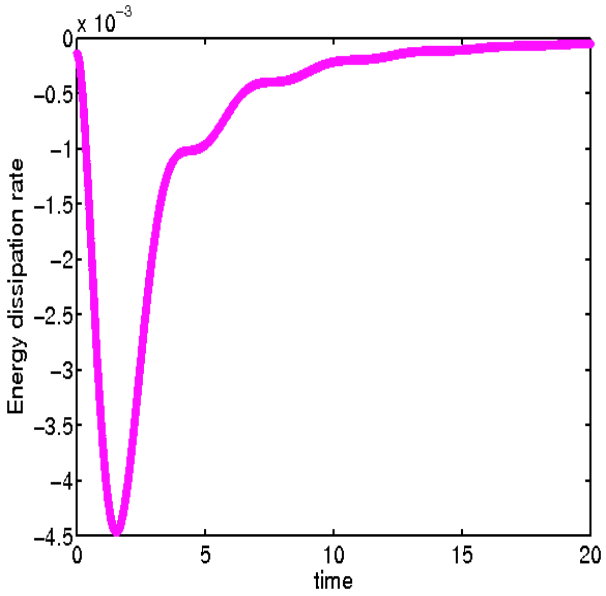

Figure 4. Evolution of energy dissipation rates in the MEDV mode turbulence. During the inital decay, the dissipation rates vary rapidly followed by a steady state where decay rates are nearly negligible and follows a Kolmogorov-like energy cascade law. The latter is consistent with Fig (3) that depicts a constancy of energy in the steady state MEDV mode turbulence.

MEDV mode turbulence the process of inverse cascade is inhibited conspicuously by the diagmanetic-like nonlinearity that depletes the large-scale flows. Furthermore, the interaction between the nonlinearity and the background inhomogeneous flows (associated $\partial_y T$ and $\partial_y B$ terms) leads to higly anisotropic nonlinear streamer-like strucutres (see Figs (1) and (2)).

Since the energy is dominated by higher k's in the MEDV mode turbulence, the inclusion of dissipation is expected to damp the turbulent energy. This is shown in Fig (3), where a significant decay of initial turbulent energy can be seen, which is followed by energy saturation in the steady state. The decay of turbulent energy is proportional to the dissipation. Thus larger is the dissipation, higher the energy decay rates are. After nonlinear interactions are saturated, the energy in the turbulence does not dissipate further and remains nearly unchanged throughout the simulations. Correspondingly, the energy transfer rate shows a significant change during the initial and nonlinear phases. However, when nonlinear interactions saturate, the nonlinear transfer of the energy in the spectral space amongst various turbulent modes becomes inefficient and the energy transfer per unit time tends to become negligibly small, as shown in Fig (4).

5. Energy spectrum

It is clear from the nonlinear structures associated with B, $\nabla^2 B$ and $B - \nabla^2 B$ that the mode structures are dominated by $k_y \approx 0$ streamer-like modes. Correspondingly, the inertial range spectrum should contain signature of the highly anisotropic streamer-like flows. One thus expects that the resultant energy spectrum might de-

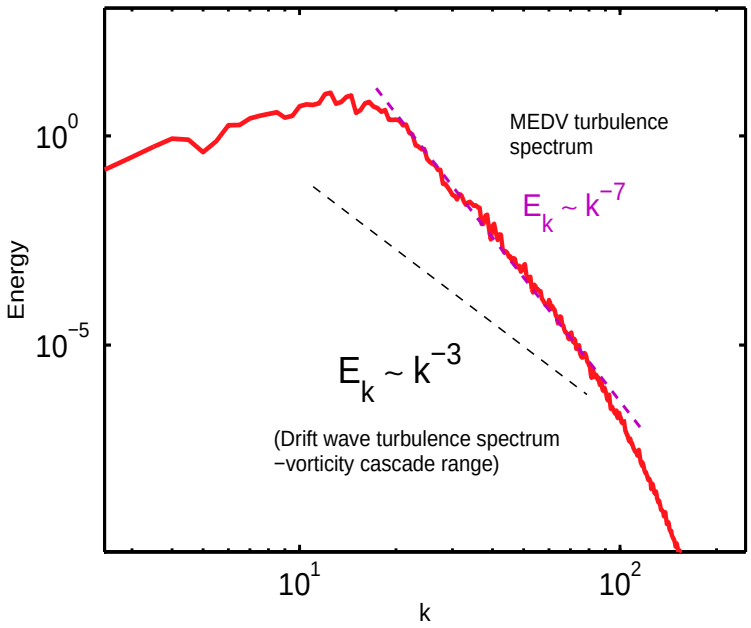

Figure 5. MEDV mode turbulence spectrum is much steeper than the usual inhomogeneous drift wave turbulent spectrum in the forward cascade vorticity regime (k^{-3}). The observed spectrum in our simulation depicts a non Kolmogorov-like k^{-7} spectrum. The underlying steepness in the inertial range spectrum is mediated by the highly anisotropic nonlinearly excited streamer-like structures for which $k_y \approx 0$.

viate from the standard Kolmogorov spectrum that is exhibited by the HM drift wave turbulence and its several variants. To investigate the spectral features of MEDV mode turbulence, we plot the inertial range energy spectrum in Fig (5). It is seen from this figure that the MEDV mode spectrum is much steeper than its usual 2D drift wave (isotropic) turbulence counterpart. The inertial range energy spectrum, in the latter, exhibits a Kolmogorov-like k^{-3} spectrum [18] in the vorticity cascade regime (see the adjacent curve in Fig (5)). The spectral index associated with the MEDV mode turbulence is close to k^{-7} in the forward cascade vorticity regime. There is a greater disparity in the two spectra. While the disparity in the MEDV mode spectrum is caused essentially by the anisotropic turbulent cascades, it is interesting to know whether it can be understood from a Kolmogorov-like phenomenology. In view of pursuing this issue, we derive the MEDV mode turbulence spectrum based on the Kolmogorov-like dimensional arguments that are described in the following.

The energy cascade is mediated essentially by the nonlinear convective forces in the MEDV mode turbulence and is proportional to kB_k, where k is a wavenumber associated with the magnetic field B_k in the spectral space. The corresponding energy transfer time can then be estimated as $\tau_{nl} \sim (kB_k)^{-1}$. The energy transfer rates, in the forward cascade vorticity regime, are determined by the vorticity per unit nonlinear time, i.e.

$$\varepsilon(k) \sim \frac{|\Omega_k|^2}{\tau_{nl}} \sim \frac{k^2|B_k|^2}{\tau_{nl}}.$$

It should be borne in mind that the energy transfer rates, described above, are influenced significantly by the presence of the propagating MEDV modes. The linear normalized frequency of this mode can be determined from the dispersion relation. The linear interaction time of EDM with nonlinear eddies, in $k \gg 1$ dispersive limit, can be given as $\tau_l \sim k/k_y$. This interaction time needs to be necessarily included in the energy transfer rates because the MEDV mode couples with nonlinear fluctuations. The modified energy cascade rates are given in the following.

$$\varepsilon(k) \sim \frac{k^2|B_k|^2}{\tau_{nl}^2}\tau_l \sim \frac{k^5|B_k|^3}{k_y}.$$

We next apply the Kolmogorov theory of turbulence that describes that the inertial range spectral cascade is local and depends on the wavenumber, as follows.

$$E_k \sim \varepsilon(k)^\alpha k^\beta.$$

On substituting the energy transfer rates in the above expression, one obtains

$$k^{-1}|B_k|^2 \sim \left(\frac{k^5|B_k|^3}{k_y}\right)^\alpha k^\beta.$$

On equating the indices of identical bases, we get $\alpha = 2/3$ and $\beta = -20/3$. This further yields a $E_k \sim k^{-20/3}$ energy spectrum in the forward cascade vorticity regime. The spectrum obtained by including the MEDV mode interaction time in the Kolmogorov phenomenology is in close agreement with (if not exactly identical to) the observed energy spectrum (see Fig (5)). More steeper spectral index can be followed *qualitatively* from the entire energy spectrum that contains the anisotropic streamer-like flows. It can be described by the following expression.

$$E_k \sim \varepsilon(k)^{2/3}k^{-20/3}k_y^{-2/3}. \tag{9}$$

Thus, the deviation from the usual Kolmogorov-like k^{-3} spectrum increases with the anisotropy. The latter can be triggered either by the presence of the mean magnetic field or background inhomogeneous flows. The spectrum described by Eq. (9) depicts a much steeper spectral slope for streamer flows that have smaller magnitude of k_y (or close to, but not entirely, zero). Note carefully that Eq. (9) does not reduce to a standard k^{-3} spectrum describing the isotropic MEDV fluctuations, because the anisotropy of the spectral cascade is introduced in the energy cascade rates through a ratio of linear and nonlinear periods. This choice does not allow us to simply reduce the former to an isotropic turbulent spectrum. In this respect, the anisotropic turbulent spectrum described by Eq. (9) is only qualitative. A quantitative spectrum discerning the dependence on k_x and k_y may require an altogether different analytic approach and is beyond the scope of the present paper.

6. Electron transport in magnetic structures

We finally estimate the electron transport in the presence of magnetic field structures created due to nonlinear interactions between the MEDV modes. In the presence of an ensemble of magnetic field structures the electrons perform a random walk and diffuse. Accordingly, there results and effective electron diffusion coefficient, D_{eff}, which can be calculated from the cross correlation of the drift speed of

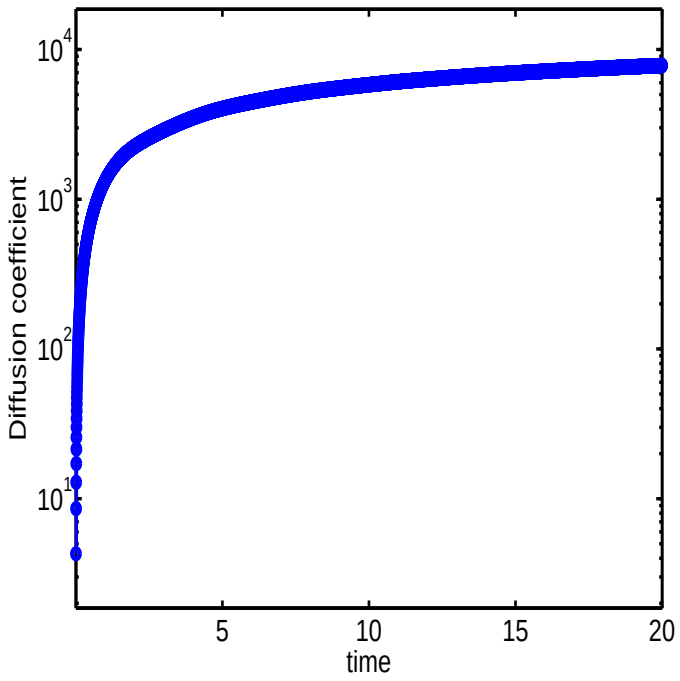

Figure 6. The MEDV mode turbulence transport is dominated by large scale streamer-like flows that are dominated by $k_y \approx 0$ modes. The electron transport is higher initially and saturates in the steady state.

the electrons in the turbulent magnetic field. We have

$$D_{eff} = \int_0^\infty \langle \mathbf{V}_\perp(\mathbf{r}, t) \cdot \mathbf{V}_\perp(\mathbf{r}, t + t') \rangle dt',$$

where the angular bracket denotes ensemble spatial averages. The perpendicular component of the electron fluid velocity associated with the MEDV mode is $\mathbf{V}_\perp = \hat{\mathbf{z}} \times \nabla B$. Since the MEDV mode turbulence is confined in the 2D plane, the effective diffusion coefficient essentially describes the diffusion processes associated with the motion of electrons that produce fluctuating magnetic fields in the $x - y$ plane. We compute the evolution of the effective diffusion caused by nonthermal magnetic fields of the MEDV modes. This is shown in Fig (6). The effective diffusion is larger during the early phase of the simulations. This is where the isotropic MEDV mode turbulence progressively evolve towards anisotropy and dominated increasingly by $k_y \approx 0$ modes. Once the anisotropic streamers are formed, they begin to saturate such that no more energy transfer takes place. The corresponding steady state transport also shows saturation. This scenario is further consistent with the evolution of energy and the subsequent decay rates depicted in Figs (3) and (4), respectively.

7. Discussion

In this paper, we have used computer simulations to investigate the properties of 2D MEDV modes in a nonuniform plasma containing the equilibrium density and electron temperature inhomogeneities. The equilibrium is maintained due to a bal-

ance between the electric force $-neE_{0x}$ and the electron pressure gradient $\partial p_0/\partial x$, where $p_0 = n(x)T_0(x)$. The electron temperature gradient can create a phase shift between the magnetic field and electron temperature perturbations, so that the MEDV mode grows provided that $\eta = d\ln T_0/d\ln n > 2/3$. Large amplitude MEDV modes interact among themselves and evolve in a turbulent state. The latter consists of magnetic filaments/streamers and localized electro heated regions in nonuniform plasmas. The resulting turbulent spectrum deviate from the usual Kolmogorov [18] or the Fyfe-Montgomery [19] scalings, which describe the complex fluid turbulence and drift wave turbulence in plasmas, respectively. Due to the random walk process, electrons would diffuse in the magnetic field structures that are created due to the nonlinear interactions between the MEDV modes. The magnetic field structures may also cause the electron heat transport on account of the electron temperature perturbation which are driven by the localized magnetic fields of the MEDV modes. The present investigation should help to understand the generation of flows, structures and associated spectra producing anomalous transport of particles and heat in inertial confinement fusion plasmas.

References

[1] Jones, R. D. 1983 Magnetic Surface Waves in Plasmas. *Phys. Rev. Lett.* **51**, 1269.

[2] Yu, M. Y. and Stenflo, L. 1985 Magnetic surface wave instabilities in plasmas. *Phys. Fluids* **28**, 3447.

[3] Stenflo, L., and Yu, M. Y. 1986 Instabilities of baroclinically driven magnetic and acoustic waves. *Phys. Fluids* **29**, 2335.

[4] Stenflo, L., Shukla, P. K., and Yu, M. Y. 1987 Decay of magnetic-electron-drift vortex modes in plasmas. *Phys. Rev. A* **36**, 955.

[5] Shukla, P. K., Yu, M. Y., and Stenflo, L. 1988 Stimulated Compton scattering of magnetic-electron-drift vortex waves off plasma ions. *Phys. Rev. A* **37**, 2701.

[6] Yu, M. Y., Shukla, P. K., and Spatschek, K. H. 1974 Scattering and modulational instabilities in magnetized plasmas. *Zh. Naturforsch. A* **29**, 1736; Shukla, P. K., Yu M. Y., and Spatschek, K. H. 1975 Brillouin backscattering instability in magnetized plasmas. *Phys. Fluids* **18**, 265; Shukla, P. K. 1978 Modulational instability of whistler-mode signals. *Nature* **274**, 874 (1978); Stenflo, L. 1970 Kinetic theory of three-wave interaction in a magnetized plasma. *J. Plasma Phys.* **4**, 585.

[7] Sharma, R. P., and Shukla, P. K. 1983 Nonlinear effects at the upper-hybrid layer. *Phys. Fluids* **26**, 87; Murtaza, G. and Shukla, P. K. 1984 Nonlinear generation of electromagnetic waves in a magnetoplasma. *J. Plasma Phys.* **31**, 423; Shukla, P. K., and Stenflo, L. 1985 Nonlinear propagation of electromagnetic waves in magnetized plasmas. *Phys. Rev. A* **30**, 2110.
Stenflo, L., and Shukla, P. K., 2000 Theory of stimulated scattering of large-amplitude waves. *J. Plasma Phys.* **64**, 353.

[8] Shukla, P. K., Yu, M. Y., Rahman, H. U., and Spatschek, K. H. 1981 Excitation of convective cells by drift waves. *Phys. Rev. A* **23**, 321; Nonlinear convective motion in plasmas. *Phys. Rep.* 1984 **105**, 227; Shukla, P. K., and Stenflo, L. 2002 Nonlinear interactions between drift waves and zonal flows. *Eur. Phys. J. D* **20**, 103.

[9] Nycander, J., Pavlenko, V. P., and Stenflo, L. et al, 1987 Magnetic vortices in nonuniform plasmas. *Phys. Fluids* **30**, 1367.

[10] Shukla, P. K., Birk, G. T., and Bingham, R. 1995 Vortex streets driven by sheared flow and applications to black aurora. *Geophys. Res. Lett.* **22**, 671.

[11] Stenflo, L. 1987 Acoustic solitary vortices. *Phys. Fluids* **30**, 3297.

[12] Jucker, M., and Pavlenko, V. P. 2007 On the modulational stability of magnetic structures in electron drift turbulence. *Phys. Plasmas* **14**, 102313.

[13] Andrushchenko, Z. N., Jucker, M., and Pavlenko, V. P., 2008, Self-consistent model of electron drift mode turbulence. *J. Plasma Phys.* **74**, 21.

[14] Hasegawa, A., and Mima, K. 1977 Stationary spectrum of strong turbulence in magnetized nonuniform plasma. *Phys. Rev. Lett.* **39**, 205; Mima, K., and Hasegawa, A. 1978 Nonlinear instability of electromagnetic drift waves. *Phys. Fluids* **21**, 81.

[15] Hasegawa, A., and Wakatani, M. 1983 Plasma Edge Turbulence. *Phys. Rev. Lett.* **50**, 682; *ibid.* **59**, 1581 (1987).

[16] Hasegawa, A. 1985 Self-organization processes in continuous media. *Adv. Phys.* **34**, 1.

[17] Horton, W., and Hasegawa, A. 1994 Quasi-two-dimensional dynamics of plasmas and fluids. *Chaos* **4**, 227.

[18] Kolmogorov, A. N. 1951 The Local Structure of Turbulence in Incompressible Viscous Fluid for Very Large Reynolds' Numbers. *C. R. Acad. Sci. U. R. S. S.* **30**, 301, and **30**, 538 (1941).

[19] Fyfe, D., and Montgomery, D. 1979 Possible inverse cascade behavior for drift-wave turbulence. *Phys. Fluids* **22**, 246.